# Influence of Hydration on Protein Dynamics: Combining Dielectric and Neutron Scattering Spectroscopy Data

**ARTICLE** *in* THE JOURNAL OF PHYSICAL CHEMISTRY B · NOVEMBER 2008

Impact Factor: 3.3 · DOI: 10.1021/jp8059807 · Source: PubMed



**3 AUTHORS**, INCLUDING:

Sheila Khodadadi
Delft University of Technology
**18** PUBLICATIONS **413** CITATIONS

SEE PROFILE

Sebastian Pawlus
University of Silesia in Katowice
**97** PUBLICATIONS **1,716** CITATIONS

SEE PROFILE

# Influence of Hydration on Protein Dynamics: Combining Dielectric and Neutron Scattering Spectroscopy Data

**S. Khodadadi,[†] S. Pawlus,[†,‡] and A. P. Sokolov*[,†]**

*Department of Polymer Science, The University of Akron, Akron, Ohio 44325, and Institute of Physics, Silesian University, ul. Uniwersytecka 4, 40-007 Katowice, Poland*

*Received: July 7, 2008; Revised Manuscript Received: August 26, 2008*

Combining dielectric spectroscopy and neutron scattering data for hydrated lysozyme powders, we were able to identify several relaxation processes and follow protein dynamics at different hydration levels over a broad frequency and temperature range. We ascribe the main dielectric process to protein's structural relaxation coupled to hydration water and the slowest dielectric process to a larger scale protein's motions. Both relaxations exhibit a smooth, slightly super-Arrhenius temperature dependence between 300 and 180 K. The temperature dependence of the slowest process follows the main dielectric relaxation, emphasizing that the same friction mechanism might control both processes. No signs of a proposed sharp fragile-to-strong crossover at $T \sim 220$ K are observed in temperature dependences of these processes. Both processes show strong dependence on hydration: the main dielectric process slows down by six orders with a decrease in hydration from $h \sim 0.37$ (grams of water per grams of protein) to $h \sim 0.05$. The slowest process shows even stronger dependence on hydration. The third (fastest) dielectric relaxation process has been detected only in samples with high hydration ($h \sim 0.3$ and higher). We ascribe it to a secondary relaxation of hydration water. The mechanism of the protein dynamic transition and a general picture of the protein dynamics are discussed.

## Introduction

Understanding how proteins function depends significantly on our understanding of protein dynamics and underlying energy landscape. Knowledge of proteins' three-dimensional structure is not sufficient. Protein even in a folded state explores an enormous number of various conformational states, and transitions between these states are essential for protein function. Yet, despite a few decades of intensive studies, our current understanding of protein dynamics even on a qualitative level remains very limited.

Protein dynamics span over an enormous frequency (time) range and include several local and collective motions from bond vibrations and methyl group rotation to loop motion and larger domain motions. It is well-known that solvents, including water of hydration, affect a protein's dynamics and activity tremendously.[1−6] Most enzymes are inactive in the dehydrated state, and their activity increases sharply with an increase in hydration.[1,4] Many publications emphasize that protein dynamics and activity are "slaved" by the solvent.[2,5,6] Moreover, there is strong evidence that protein and solvent dynamics are strongly coupled even on picosecond−nanosecond time scales.[7] Nevertheless, details of the protein−solvent interactions and the role of hydration in protein dynamics and activity remain poorly understood.

Many experimental techniques have been used to study protein dynamics. NMR provides detailed information on local motions of particular groups (e.g., methyl groups).[8,9] However, it misses the information on larger scale global motions. Neutron spectroscopy can provide very important information on microscopic details of molecular motions, including the geometry of atomic motions on various length scales, through analysis of scattering wave-vector dependencies.[10] However, the experimentally accessible frequency window of neutron spectroscopy is limited and allows study of the protein dynamics mostly on picosecond−nanosecond time scale. Dielectric spectroscopy provides an extremely broad frequency range but suffers from difficulties in interpretation of the data. Dielectric measurements do not provide any microscopic information, and even assignment of the relaxation modes (whether it is the mode of a protein or of a solvent) is not obvious.[11−14] Molecular dynamics (MD) simulations are probably the best approach to visualize the protein's motions (as long as we can trust the model). However, they are also limited to rather fast time scales (nanoseconds) and a very small ensemble of molecules. It is obvious that the most successful approach is a combination of various experimental techniques that can complement one another and provide better justification for experimental data interpretations.

The current contribution presents combined dielectric and neutron scattering data of lysozyme's dynamics at different levels of hydration in a broad temperature and frequency range. Dielectric spectroscopy identifies three relaxation processes. Comparison to neutron scattering data helps to assign the processes: the main process at intermediate frequencies is ascribed to a coupled protein−water structural relaxation and the weak fast process to a local relaxation in water of hydration. The microscopic nature of the slowest dielectric process (which is outside of the frequency range of neutron spectrometers) remains unclear. The main relaxation process exhibits a smooth, slightly super-Arrhenius temperature dependence between $T \sim 300$ K and $T \sim 180$ K. We also demonstrate that the sharp rise in mean-squared atomic displacements $\langle r^2 \rangle$ of hydrated protein observed in neutron scattering experiments at $T \sim 200-230$ K (the so-called dynamic transition[15,16]) is caused by the protein's relaxation time reaching the resolution window of the neutron spectrometer. Protein dynamics exhibit no peculiar behavior at this temperature range. The relaxation time of the slowest

* Corresponding author. E-mail: alexei@uakron.edu.
[†] The University of Akron.
[‡] Silesian University.

10.1021/jp8059807 CCC: $40.75 
Published on Web 10/23/2008

process follows the main relaxation process. The characteristic relaxation time of both processes slows down significantly with a decrease in hydration, but the slowest process exhibits a stronger dependence on hydration.

## Experimental Section

**Samples and Measurements.** Hen egg white lysozyme (from Sigma-Aldrich) was dialyzed, to remove salts, and lyophilized. The lyophilized sample has residual hydration $h \sim 0.05$ (grams of water per 1 g of protein) and was used as a dry sample. Isopiestic equilibration of lyophilized lysozyme above the saturated NaCl solution resulted in hydration levels of $h = 0.1$, 0.18, and 0.23. Higher hydration levels were achieved by isopiestic equilibration of dry powder above the open water in closed volume (100% rh). The final hydration levels were estimated by thermogravimeric analysis.

Dielectric spectra in the frequency range between $10^{-2}$ and $10^9$ Hz were measured using the Concept 80 system from Novocontrol (the low-frequency range, $\nu < 10^7$ Hz, was measured using a Novocontrol Alpha-analyzer, and the high-frequency range, $\nu > 10^6$ Hz, was measured using an Agilent 4291B impedance analyzer). Samples were placed between two gold-coated parallel-plate electrodes. Teflon was used as a spacer. To minimize evaporation of water, an external Teflon ring was used to seal the samples. A capacitor with the sample was placed in a cryostat. Temperature was stabilized better than 0.1 K by a nitrogen gas flow using a Novocontrol Quatro temperature controller. After the cycle of temperature measurements, we repeat the initial temperature measurement to see reproducibility and repeatability of the measurements. Weighing the samples before and after the measurements did not show any significant weight changes, indicating that hydration was kept constant during the measurements.

Neutron scattering data for lysozyme hydrated with $D_2O$ have been obtained using the high-flux backscattering and the time-of-flight disk chopper spectrometers at the National Institute of Standards and Technology and the new back-scattering spectrometer at Spallation Neutron Source at the Oak Ridge National Laboratory. More details about the measurements and data analysis have been presented in previous publications.[17,18] One of the advantages of neutron scattering spectroscopy is the extremely high cross section of hydrogen atoms. As a result, neutron scattering spectra of lysozyme/$D_2O$ reflect primarily the motion of lysozyme's nonexchangeable hydrogen atoms. Contribution of water is negligible. This high contrast between H and D atoms provides clear assignment of the relaxation processes observed in neutron scattering spectra.

***Analysis of the Dielectric Relaxation Spectra.*** Figure 1 presents the real and imaginary parts of the complex dielectric permittivity $\varepsilon^*(\nu)$ spectra of dry and hydrated lysozyme at a few selected temperatures. Spectra of the dry sample show a single relaxation peak (Figure 1b). In the hydrated sample, the spectra of $\varepsilon''(\nu)$ show a tail of conductivity at lower frequencies, the main relaxation peak, that splits in two at lower temperatures, and some indication of another process between the conductivity and the main process (Figure 1d). This slowest process overlaps strongly with the conductivity tail, but its presence is clear in the derivative analysis of the real part of permittivity (see Appendix A). Detailed analysis of the spectra was performed using WINFit software from Novocontrol. The spectra were fit by a few (up to three) Cole−Cole (CC) distribution functions plus a conductivity tail:

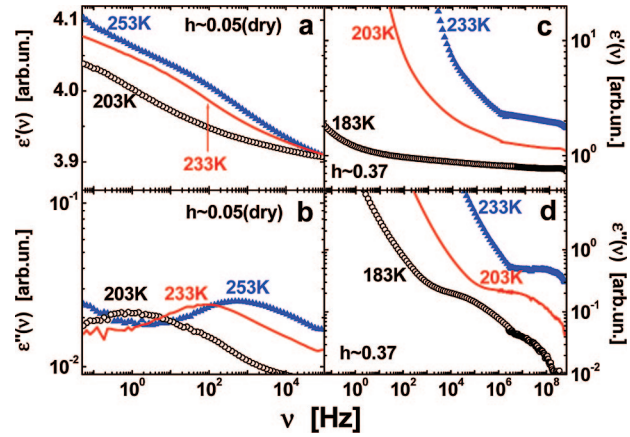


**Figure 1.** Spectra of real $\varepsilon'(\nu)$ and imaginary $\varepsilon''(\nu)$ parts of the dielectric permittivity of dry (a, b) and hydrated (c, d) lysozyme samples at a few selected temperatures. Only one relaxation process is observed in the spectra of dry lysozyme ($h = 0.05$). However, up to three relaxation processes are observed in the spectra of hydrated protein ($h = 0.37$).

$$\varepsilon^* = \varepsilon_\infty + \sum_j \frac{(\Delta\varepsilon)_j}{1 + (i\omega\tau_j)^{\alpha_j}} - i\frac{\sigma}{\varepsilon_0\omega^s}, \quad j = 1,2,3 \quad (1)$$

Here, $\omega = 2\pi\nu$ is the angular frequency, $\tau_j$ is the relaxation time, $\Delta\varepsilon_j$ is the dielectric strength, and $\alpha_j$ is the stretching parameter of the $j$ relaxation process, $\sigma$ presents the amplitude of the conductivity tail, and $s$ is the exponent describing the tail slope. Details of the fit procedure are presented in Appendix A. Figure 2a presents an example of the fit spectra for a hydrated sample. We also analyzed the temperature dependence of DC conductivity (Figure 2b) in samples with the highest hydration.

## Results

Detailed analysis of the dielectric spectra reveals three relaxation processes in lysozyme at high hydrations $h \sim 0.37-0.3$ (Figure 2a) and temperatures below ~220 K. There are only two processes at higher temperatures because the main and the fastest processes merge around $T \sim 220-225$ K. Two processes have been observed at intermediate hydrations $0.1 < h < 0.3$ (the fastest process was not detectable) and only one process at low hydrations $h \sim 0.1$ and $h \sim 0.05$ (Figure 1). Characteristic relaxation times of these processes were estimated from the frequency of the maximum in $\varepsilon''(\nu)$ of the fit curves, $\tau = (2\pi\nu_{max})^{-1}$ (Figure 2a). Figure 3 shows the temperature dependence of relaxation times in hydrated lysozyme at $h \sim 0.37$. The main relaxation process shows smooth, slightly super-Arrhenius temperature variations in the temperature range from 253 K down to $T \sim 180$ K. The characteristic relaxation time of the slower process is separated from the main process by approximately 3 orders, but it shows a similar temperature dependence (Figure 3). In contrast, the fastest process shows much weaker, Arrhenius-like temperature dependence. This kind of behavior is typical for some local secondary relaxations in complex systems. Figure 3 compares the estimated dielectric relaxation times for hydrated lysozyme to the data from neutron scattering spectroscopy. Neutron scattering on lysozyme/$D_2O$ provides information on structural relaxations of lysozyme, and contribution of hydration water to the spectra is negligible.[10,19] In contrast, the differential spectra of lysozyme/$H_2O$ and lysozyme/$D_2O$ samples provide information primarily on relaxation of water of hydration.[20] Surprisingly, dielectric relaxation data for the main process are very similar to the neutron

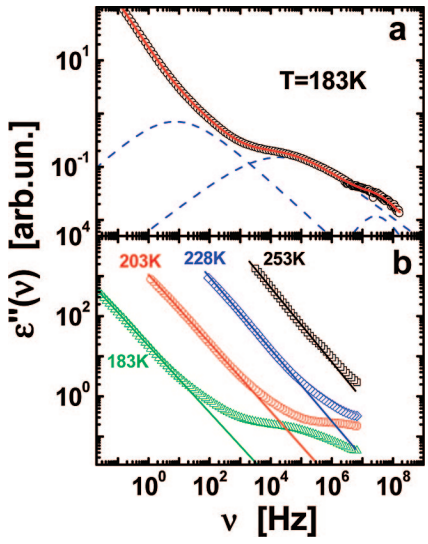


**Figure 2.** (a) Dielectric loss spectrum of hydrated lysozyme ($h \sim 0.37$) at $T = 183$ K (symbols) and its fit to eq 1 (solid line). Dashed lines show spectra of the three relaxation processes. (b) Conductivity tail in the $\varepsilon''(\nu)$ spectra of hydrated lysozyme ($h \sim 0.37$) at a few selected temperatures (symbols) and their fit by a power law $\varepsilon''(\nu) \propto \nu^{-1}$ (solid lines).

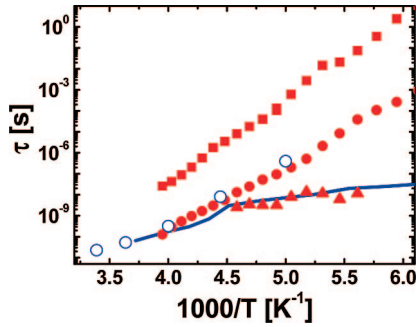


**Figure 3.** Temperature dependence of characteristic relaxation times of the three dielectric processes in the hydrated ($h = 0.37$) sample: (●) the main, (▲) the fastest, and (■) the slowest processes. The fastest process splits from the main process at $T \sim 220-225$ K. The ○ symbol presents the protein's relaxation time for hydrated ($h \sim 0.4$) lysozyme estimated from neutron scattering experiments (data from ref 18); the solid line presents the relaxation time for the lysozyme's hydration water estimated from neutron scattering experiments (data from ref 20).

scattering data for structural relaxation in lysozyme. At the same time, the dielectric data for the fastest process appear to be similar to the low-temperature neutron scattering data for water of lysozyme hydration (Figure 3).

Figure 4 shows temperature dependences of the relaxation times estimated from the dielectric measurements at different hydration levels. Decrease in hydration leads to significant slowing down of the main and the slower relaxation processes. However, the slope of their temperature dependence does not change appreciably with hydration. Different behavior is observed for the fastest dielectric process. Its relaxation time does not show significant dependence on hydration (Figure 4a), but its amplitude decreases with a decrease in $h$ and it becomes undetectable at $h < 0.3$.

## Discussion

**I. Assignments of the Dielectric Relaxation Processes.** Dielectric spectra of proteins in solutions have been studied for many years. The rotational contribution of proteins (tumbling)

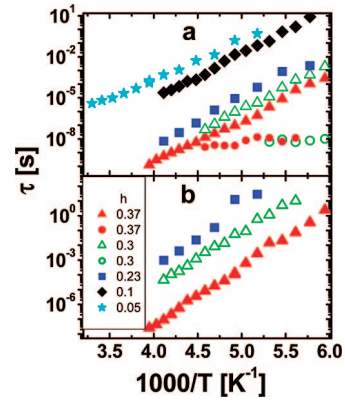


**Figure 4.** Temperature dependence of the characteristic relaxation time for the main process (a) and for the slowest process (b) in samples with different hydrations. In addition, part (a) presents the relaxation times of the fastest process at $h = 0.37$ (closed circles) and at $h = 0.3$ (open circles). This process is not detectable in the spectra of samples with lower hydrations.

and the contribution of bulk water dominate the dielectric relaxation spectra of solutions and have been clearly identified.[12,13] At ambient temperature, protein tumbling usually appears at 1−10 MHz frequencies and is called $\beta$-relaxation, while bulk water peak appears at $\nu \sim 20$ GHz and is usually called $\gamma$-relaxation.[13] There are several (up to three are reported in ref 13) weaker dielectric processes in the frequency range between the $\beta$- and $\gamma$-processes. They are called $\delta$-processes, and their interpretation remains controversial. $\beta$- and $\gamma$-processes should not contribute to our dielectric spectra because protein rotation is strongly slowed down and there is no bulk water at hydration levels of $h \sim 0.37$ and lower.

Let us start our analysis from the fastest relaxation process that splits from the main process at $T \sim 220$ K (Figures 3 and 4a). This process has also been detected in hydrated myoglobin.[21] According to our measurements, this process disappears (becomes undetectable) at hydration levels below $h \sim 0.3$. We also do not see any traces of this process in neutron scattering spectra of lysozyme/$D_2O$ (Figure 3).[19] These results suggest that the process is not related to protein relaxation but rather to water of hydration. Indeed, a process with similar relaxation time and temperature variations has been detected in water of lysozyme hydration by neutron spectroscopy (Figure 3).[20] In that case, the authors[20] used detailed comparison of lysozyme/$H_2O$ and lysozyme/$D_2O$ spectra to study the dynamics of water of hydration. A good agreement between the neutron scattering data for water of hydration and our dielectric measurements support the assignment of this process to water of hydration. According to the neutron scattering studies,[20] characteristic relaxation time of this process is essentially independent of the scattering wave vector Q, indicating that it is a local relaxation process. Its Arrhenius temperature dependence with relatively low activation energy barrier (Figure 3a) supports this indication. Probably, it is some kind of a secondary relaxation process that exists in water of protein hydration and also in confined water (see, e.g., ref 21).

Assignments of the main and of the slower relaxation processes are not obvious. Two similar processes have been observed in dielectric spectra of hydrated myoglobin powders[22] and of protein solutions.[13] The main process is traditionally ascribed to water of protein hydration.[11−14] Strong hydrogen bonding of water molecules to the protein surface leads to slowing down of dynamics of hydration water. Similarity of the relaxation time of the main process with the dielectric

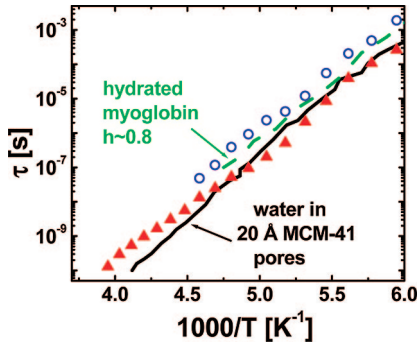


**Figure 5.** Temperature variations of the main dielectric relaxation process at $h \sim 0.37$ (▲) and $h \sim 0.3$ (○). The solid line presents literature data for the dielectric relaxation in water confined in 20 Å pores of MCM-41 glass (data from ref 21). The dashed line presents the dielectric relaxation process in hydrated myoglobin at $h \sim 0.8$ (data from ref 22).

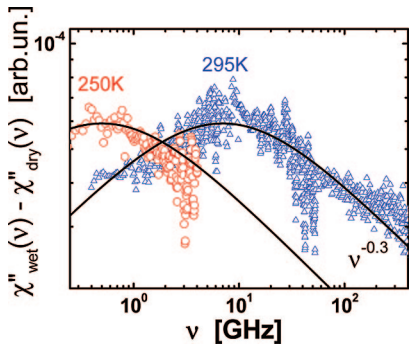


**Figure 6.** Neutron scattering susceptibility spectra of the structural relaxation in hydrated lysozyme ($h \sim 0.4$) at two selected temperatures (symbols) (data from ref 18). The spectrum at each temperature is obtained by a subtraction of the spectrum of dry protein ($h \sim 0.03$) from the spectrum of hydrated protein in order to correct for the methyl group contributions (for details, see ref 19). The solid lines represent the fit by CC distribution function with the stretching parameter $\alpha = 0.3$.

relaxation time measured in confined water (Figure 5) is consistent with this interpretation. However, the dynamics of confined water depends strongly on the degree of confinement[22] and the main dielectric process in our measurements also depends strongly on hydration level of lysozyme (Figure 4a). So, it is not obvious whether agreement between our data at $h \sim 0.37$ and water confined in 20 Å pores of MCM-41 glass is not a coincidence.

It is known that neutron scattering spectra of lysozyme/$D_2O$ samples reflect motion of protein and the contribution of hydration water is negligible at hydration levels of $h \sim 0.37$ and lower.[10,19] Figure 6 presents neutron scattering susceptibility spectra $\chi''(\nu)$ (analogous to dielectric loss spectra) for the main structural relaxation of lysozyme at $h \sim 0.4$. The spectra exhibit extremely strong stretching with CC parameter $\alpha \sim 0.3$. The temperature dependence of the characteristic relaxation time of this process is shown in Figure 3. It appears that the relaxation time of lysozyme estimated from the neutron scattering spectra agrees well with the relaxation times of the main dielectric process. Both processes exhibit identical temperature dependence (Figure 3). Moreover, the spectral shape (the stretching parameter) of the main dielectric relaxation process (Figure 7) is similar to the lysozyme relaxation process observed in neutron scattering spectra (Figure 6). All of these observations suggest that the same relaxation process might be observed in neutron and in dielectric studies. It would mean that the main dielectric

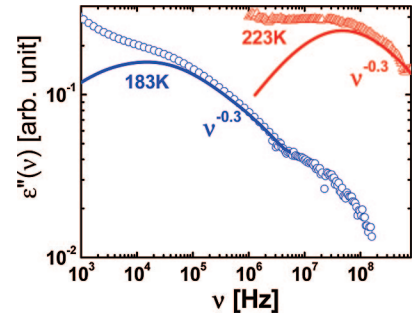


**Figure 7.** Spectra of the main dielectric relaxation process in hydrated ($h = 0.37$) lysozyme (symbols) exhibit stretching similar to the one observed in neutron scattering spectra (Figure 6). The solid lines show fit by CC distribution function with the stretching parameter $\alpha = 0.3$.

process includes structural relaxation of a protein. This assignment is consistent with the strong hydration dependence of this process: It slows down by ~6 orders with decrease in hydration, and is clearly visible even at extremely low hydration levels (Figures 1b and 4a).

According to the neutron scattering data, the averaged structural relaxation time of lysozyme at ambient temperature is $\tau \sim 25$ ps (Figure 3). Extremely strong stretching of this process suggests broad distribution of relaxation times in this picosecond range. In addition, detailed NMR studies of lysozyme reveal that most of protein's side chains have a relaxation time in the range ~10−60 ps.[9] So, there is much experimental evidence of protein's relaxations in this time range, the usual range of the fastest $\delta$-process observed in protein solutions.[13,23] For example, $\tau \sim 35$ ps of the fastest $\delta$-process at ambient temperature has been reported for an aqueous solution of RNaseA[13] and $\tau \sim 40$ ps for an aqueous solution of myoglobin.[23] This observation once again emphasizes the similarity between the protein's relaxation observed in neutron scattering and the $\delta$-process observed in dielectric spectra. However, the fastest $\delta$-process is traditionally ascribed to water molecules hydrogen-bonded to the protein.[11−14] Moreover, recent MD simulation analysis[24] demonstrated that water of lysozyme hydration indeed has $\tau$ in the same range and the relaxation spectrum has strong stretching (stretching parameter ~0.3). We emphasize that our analysis cannot exclude the assignment of the main dielectric relaxation process to water of hydration. It is known that the dynamics of water and of the protein are strongly coupled. For example, MD simulations revealed a strong coupling between motion of water, water−protein hydrogen-bonding lifetime, and protein structural relaxation.[25] This strong coupling can lead to a single relaxation process that involves both hydration water and protein and will result in similar spectral shapes, relaxation times, and their temperature variations. So, we suggest that this dielectric process is not just water of hydration; instead, it reflects a coupled protein−hydration water relaxation process that involves motion of both protein and hydration water. Detailed MD simulations can help to resolve the microscopic picture of the main dielectric process. Regardless of that, the temperature dependence of this dielectric process apparently reflects the temperature dependence of the protein's structural relaxation.

Interpretation of the slower relaxation process is also controversial.[11−14] It has been observed in hydrated myoglobin[22] and in aqueous solutions of many proteins.[11−13] Many authors assigned it to water of hydration that is extremely tightly bounded to the protein surface. However, simulations and NMR studies demonstrate that hydration water molecules are moving

on a time scale that is only 2−3 times slower than the bulk water.[13,26,27] Moreover, translational motion of almost all the hydration water molecules happens on a time scale of ∼10−50 ps.[13,24,27] So, this process cannot be ascribed directly to water of protein hydration (for a detailed discussion, one can see refs 11, 13). The observed extremely strong slowing down of this process with dehydration (Figure 4b) supports this conclusion.

It is known that protein exhibits conformational fluctuations, side group motions, bending of helices, and many other intramolecular motions on time scales from picoseconds to nanoseconds. Thus, it is reasonable to ascribe the slower process to intramolecular motions of proteins.[14] It would probably represent larger scale, more global protein motion in comparison to protein's structural relaxation observed in neutron scattering spectra at $\tau \sim 25$ ps (Figures 3 and 6). In particular, it is known that the dipole moment accumulates along the α-helix.[28] Motion of this accumulated dipole will be much slower than motion of dipoles of individual residues. Thus, the slowest process might present motions of secondary structures. However, one cannot exclude that the slowest process in dielectric spectra can be a result of a cross-term in dielectric relaxation of dipoles of hydration water and of protein's dipoles, as has been proposed in refs 11, 13. Detailed simulations and neutron scattering measurements on properly hydrated/deuterated samples should be able to disentangle this problem.

**II. The Protein Dynamic Transition.** Combining neutron and dielectric spectroscopy measurements (Figure 3), we can analyze the protein's structural relaxation in a broad temperature range. This helps to unravel the microscopic mechanism underlying the so-called protein dynamic transition.[15,16,29,30] The latter appears in hydrated biomolecules as a sharp rise in mean-squared atomic displacements $\langle r^2 \rangle$ with an increase in temperature at $T$ above ∼200−230 K.[15,16] It is known that the dynamic transition is suppressed in dry proteins and it is shifted to higher temperature ($T_D \sim 270-280$ K) in protein placed in glycerol.[15,16] Although the dynamic transition has been observed in Moessbauer and neutron scattering measurements two decades ago,[15,30] its explanation still remains a subject of controversial discussions.[18−20,29−33]

Recently, Chen and co-workers performed detailed studies of water of lysozyme, RNA, and DNA hydration.[20,34,35] They observed a sudden change in the temperature dependence of the characteristic relaxation time at $T \sim 220$ K (see, e.g., Figure 3). This change has been ascribed to a phase transition in water of hydration and was named a fragile-to-strong crossover.[20] The authors suggest that this sharp change in behavior of hydration water is the cause for the protein dynamic transition.[20]

Our combined dielectric and neutron scattering data demonstrate that the protein's structural relaxation exhibits smooth temperature variations in the entire range from 295 K down to 180 K. No sudden change in the temperature dependence of its $\tau$ is observed around $T \sim 220$ K (Figures 3 and 8). The same important conclusion can be drawn from the temperature dependence of conductivity $\sigma$ (Figures 2b and 8). $\sigma$ in hydrated protein sample is related to diffusion of ions. Its temperature dependence reflects the temperature variations of the ions' diffusion coefficient and is related to the temperature dependence of structural relaxation time through the Debye−Stocks−Einstein (DSE) relationship:[36]

$$\sigma\tau = \frac{\text{const}}{T} \tag{4}$$

where the constant value depends on the concentration of ions and their size.[37] Temperature dependence of the inverse

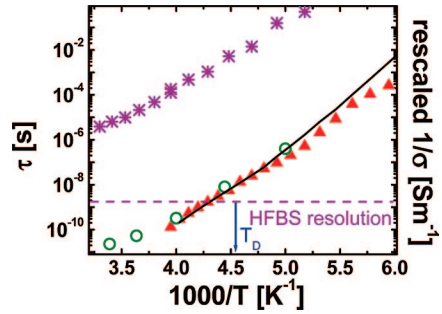


**Figure 8.** Temperature dependence of the characteristic relaxation times: (○) the protein's structural relaxation at $h \sim 0.4$ estimated from neutron scattering measurements; (▲) the main dielectric process in hydrated protein at $h = 0.37$; (∗) the main dielectric process in dry protein ($h = 0.05$). The solid line shows the temperature dependence of the inverse conductivity in hydrated lysozyme. The dashed line marks the resolution window of the neutron back-scattering spectrometer (HFBS) at NIST, and the arrow indicates the dynamic transition temperature of hydrated lysozyme, $T_D$.

conductivity in hydrated lysozyme sample is presented in Figure 8. It exhibits a smooth, slightly super-Arrhenius behavior that agrees with the temperature dependence of the main dielectric process.

Thus, the temperature dependences of protein's structural relaxation and of the ions' translational motion do not show any particular changes around $T \sim 220$ K. This result contradicts the interpretation of Chen and co-workers that structural relaxation of hydration water exhibits a strong change in behavior at $T \sim 220$ K.[20] It is not possible that such a sharp change in the structural relaxation of hydration water will not show up in the temperature dependence of conductivity or dielectric relaxation process (Figure 8). The only reasonable explanation for this contradiction is that the process measured in neutron scattering spectra of hydrated water at $T < 220$ K in refs 20, 34, 35 is not the structural relaxation but is a secondary relaxation. This explanation has been proposed earlier in refs 21, 38 and agrees well with our observation of the weak dielectric process that splits from the main process at $T < 220$ K (Figures 1−3). Thus, our results show no signs of the sharp fragile-to-strong crossover in hydrated lysozyme. Instead, the results are consistent with a split of a secondary relaxation in protein's hydration water. These results exclude the explanation proposed by Chen and co-workers of the protein dynamic transition.

As has been shown in refs 15, 19, 39, the sharp rise in $\langle r^2 \rangle$ is associated with a strong increase in quasielastic scattering intensity in neutron scattering spectra. It means that the dynamic transition is associated with some relaxation process. Our results demonstrate that the main structural relaxation approaches the resolution window of the neutron scattering spectrometer around the dynamic transition temperature (Figure 8). This observation provides a clear and in some sense trivial explanation for the sharp rise of $\langle r^2 \rangle$: It is caused by the protein's structural relaxation that reaches the neutron spectrometer resolution window. This conclusion is consistent with earlier ideas presented in refs 32, 33. We also emphasize that the main relaxation process in dry protein appears to be ∼6 orders slower than the main relaxation in hydrated protein (Figure 8). As a result, this process does not enter the neutron spectrometer resolution at any reasonable temperature. This explains the absence of the dynamic transition in dehydrated biomolecules.

**III. Influence of Hydration.** Change in the hydration level affects all three processes in the dielectric spectra. The fastest process does not change significantly its characteristic $\tau$ between

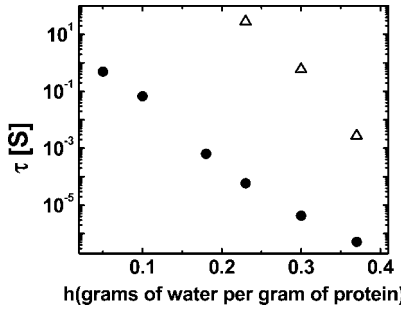


**Figure 9.** Hydration dependence of the characteristic relaxation time for the main (●) and for the slowest (△) processes at $T = 193$ K.

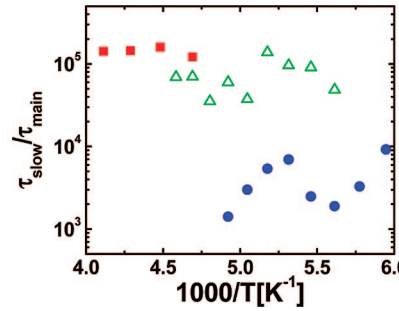


**Figure 10.** The ratio of $\tau_{slow}/\tau_{main}$ at different temperatures and hydrations: (●) $h = 0.37$; (△) $h = 0.3$; (■) $h = 0.23$.

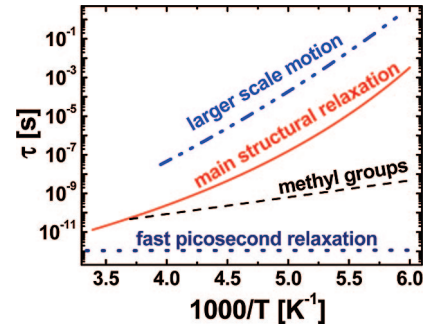


**Figure 11.** Schematic presentation of the proposed main components in dynamics of hydrated protein and their temperature dependence.

$h \sim 0.37$ and $h \sim 0.3$ (Figure 4a). However, its amplitude decreases and the process becomes undetectable at hydration levels below $h \sim 0.3$. This observation is consistent with assignment of the process to water of protein hydration.

Different behavior is observed for the main and slowest dielectric processes. Their characteristic relaxation times slow down significantly with a decrease in hydration (Figure 4). The main process, however, remains well visible even in the dry sample. It is interesting that the temperature dependence of the main dielectric process does not change much with hydration (Figure 4a). It means that the apparent activation energy of this process has rather weak hydration dependence, at least in the hydration range studied. Instead, there is a strong shift of the whole temperature dependence to longer relaxation times with a decrease in hydration. Figure 9 presents the hydration dependence of characteristic $\tau$ for the main and slowest processes measured at $T = 193$ K.

Such a strong slowing down of the main dielectric process with a decrease in hydration supports the proposed assignment of this process to the protein structural relaxation couple to water of hydration. It is difficult to expect that relaxation of protein's hydration water alone will slow down a million times upon a decrease in hydration. At the same time, reduction of hydration might slow down protein relaxation by many orders due to a simple plasticizing effect. The microscopic mechanism of the protein structural relaxation observed in neutron scattering remains unknown.[19,40] It cannot be ascribed to motions of loops because almost all protein's hydrogen atoms are involved in this motion.[19] NMR relaxation studies show[9] that side groups in lysozyme move on the same time scales of ~10−60 ps. However, it is not clear how much motion of the backbone is involved in this structural relaxation. Analysis of the neutron scattering spectra suggests that the involved motions of hydrogen atoms are restricted to a radius of ~3 Å.[19] Neutron scattering studies at ambient $T$ demonstrate the strong decrease of the contribution of this process to the quasielastic scattering spectra with decrease in hydration.[19,39] This observation is consistent with the strong slowing down of the main dielectric process (Figure 9). Unfortunately, neutron scattering studies were performed at room temperature only and their direct comparison to our dielectric spectroscopy data is not possible. The latter do not cover the high-frequency range required for the comparison with neutron scattering data at room temperature.

The amplitude of the slowest process also does not change much with hydration, but it disappears from our frequency window at lower $h$ due to significant slowing down of the process (Figure 4). We were not able to analyze this process at hydrations lower than $h \sim 0.2$. Both the hydration and temperature dependences of the slowest process are similar to the ones of the main process (Figure 4). To provide a more accurate comparison, we analyzed the ratio of $\tau_{slow}/\tau_{main}$ at different temperatures and hydrations (Figure 10). The comparison reveals that the ratio of the relaxation times remains almost constant with temperature, demonstrating the same temperature dependence for both processes. Thus, the same activation barriers or the same friction mechanism control both processes. However, the separation between these two processes increases with a decrease in $h$ (Figure 10), indicating stronger dependence of the slow process on hydration.

On the basis of the experimental results presented here and earlier literature data,[14,19,22] we propose the following sketch of the protein dynamics and its hydration dependence (Figure 11). There is the fast picosecond relaxation characteristic for dynamics of all soft materials. It reflects small-scale conformational fluctuations that are usually ascribed to a rattling of structural units (amino acid residues for proteins) in a cage formed by neighbor units (residues and water molecules).[19] This process is considered to be a precursor of the larger scale structural relaxation processes. It appears in neutron and light scattering spectra in the frequency range ~100 GHz−1 THz.[19] The amplitude of this process in proteins increases significantly with hydration at $h < 0.2$.[19] It is strongly coupled to the fast relaxation of the solvent molecules and is strongly suppressed at lower temperatures.[7] Methyl group rotation is another example of the fast components of protein dynamics.[19,41−43] It has a rather low energy barrier with broad distribution of barriers.[19,42,43] According to detailed NMR, neutron, and MD simulation studies, methyl group dynamics is essentially independent of hydration.[19,42,43] There are many other side group motions. They might also be independent of hydration if they are buried deep in the hydrophobic core. Another important process is the protein's structural relaxation. It has a slightly super-Arrhenius temperature dependence and is the main cause for the sharp rise in atomic $\langle r^2 \rangle$ at $T$ above ~200−220 K (the dynamic transition). This process might present cooperative motions of amino acids between different conformational states strongly coupled to motions of hydration water. It depends strongly on $h$ and slows down significantly upon dehydration. However, its

dependence on hydration essentially saturates at $h \sim 0.5$ and might have no significant variations between $h \sim 0.5$ and dilute solution.[19] The slower process might represent larger scale motions, e.g., kinds of hinge-bending or domain motions. Its dependence on hydration is even stronger than the hydration dependence of the main structural relaxation, but its temperature dependence seems to follow the main structural relaxation. Detailed MD simulation studies combined with advanced neutron scattering measurements should help to unravel the microscopic details of these two processes.

## Conclusion

We studied the influence of hydration on lysozyme dynamics by combining dielectric relaxation data with earlier neutron scattering results. Three different processes have been identified in the dielectric relaxation spectra of hydrated lysozyme. The fastest process is only detectable at $h \sim 0.37$ and 0.3, and we ascribe it to a secondary relaxation of the protein's hydration water. The main dielectric process is traditionally assigned to water of hydration. However, comparison to neutron scattering data suggests that this process might be related to a coupled protein−hydration water structural relaxation. Our results reveal no signs of the cusplike fragile-to-strong crossover at $T \sim 220$ K postulated in ref 20, neither in the protein's structural relaxation nor in its hydration water. The protein's structural relaxation exhibits a smooth, slightly non-Arrhenius temperature dependence, and when it reaches the frequency window of the neutron spectrometer, it causes a sharp rise in the measured mean-squared atomic displacements $\langle r^2 \rangle$. Thus, the protein dynamic transition is caused by this relaxation process entering the resolution window of the neutron spectrometer. This process slows down significantly with a decrease in hydration. Assignment of the slowest relaxation process is not obvious, but it is most probably related to larger scale protein motions, e.g., hinge-bending, secondary structure, or domain motions. Its temperature dependence is similar to the temperature dependence of the main relaxation process, but it exhibits a much stronger hydration dependence. Detailed MD simulations and neutron scattering studies can help to unravel the microscopic nature of these two processes and their possible connection to protein's function.

## Appendix A: Fit of the Dielectric Spectra

We fit the dielectric spectra of lysozyme at low hydrations ($h = 0.1$ and $h = 0.05$) by a single CC distribution function plus a low-frequency tail (representing the conductivity). Analysis of the $\varepsilon''(\nu)$ spectra of hydrated samples with strong conductivity contribution and many (up to three) overlapping relaxation processes is more complicated. Since conductivity does not contribute to the real part of $\varepsilon^*$, it is more efficient to analyze the real part of the dielectric permittivity. According to the Kramers−Kronig relationship, $\varepsilon'(\nu)$ contains the same information about relaxation processes as $\varepsilon''(\nu)$.[44] In first approximation,

$$\varepsilon'' \propto -\frac{2}{\pi}\frac{\mathrm{d}\varepsilon'}{\mathrm{d}\log\nu} \tag{1a}$$

The slower relaxation process is more clearly visible in this presentation than in $\varepsilon''(\nu)$ (Figure 12). First, we fit the $-2\,\mathrm{d}\varepsilon'/\pi\,\mathrm{d}\log\nu$ spectra in the frequency range $10^{-2} < \nu < 10^{7}$ Hz by a sum of two CC distribution functions and the low-frequency tail (in that case presents some contact polarization effect). As the next step, we use the real part $\varepsilon'(\nu)$ of the permittivity

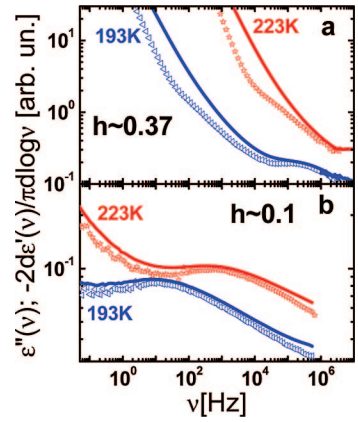


**Figure 12.** Illustrative examples of the dielectric loss spectra $\varepsilon''(\nu)$ (solid lines) and of the derivative of the real part, $-2\,\mathrm{d}\varepsilon'/\pi\,\mathrm{d}\log\nu$ (symbols), of hydrated lysozyme (a) and of dehydrated lysozyme at $h = 0.1$ (b). Relaxation processes are more pronounced in the derivative spectra.

spectra, corrected for the contact polarization effect (subtracted a power law at low frequencies). We fit the corrected $\varepsilon'(\nu)$ spectra by a sum of two CC distribution functions with values of $\tau_{slow}$ and $\tau_{main}$ fixed to the values from the previous fit and set all other parameters free. After that, we fixed the shape parameters $\alpha_{slow}$ and $\alpha_{main}$ to the values from the previous fit, and fit the $\varepsilon'(\nu)$ spectra by a sum of two CC functions with all other parameters set free. We continue this iteration procedure until the fit parameters stop to vary. At higher temperatures, when the main process moves to higher frequency range ($\nu > 1$ MHz), we joined high- and low-frequency $\varepsilon'(\nu)$ spectra and fit them by a sum of two CC functions using the iteration procedure similar to the one used at lower frequencies. At the end, we fit the $\varepsilon'(\nu)$ spectra by a sum of two CC functions with all the parameters set free.

A more complex procedure has been used to fit the spectra of hydrated samples ($h = 0.37$ and $h = 0.3$) at $T < 223$ K, because the additional fast process splits from the main process in this temperature range (Figures 1 and 2). In that case, we used combined high- and low-frequency spectra of $\varepsilon''(\nu)$ and fit them by a three CC distribution function and a conductivity tail (eq 1) with the relaxation times $\tau_{slow}$ and $\tau_{main}$ and their stretching parameters fixed to the values obtained from the previous fit of the $\varepsilon'(\nu)$ spectra. Then, we used combined $\varepsilon'(\nu)$ spectra and fit them by a sum of three CC functions with all the parameters free and their initial values set to the results of the previous fit.

The described above iteration procedure was essential for the estimates of the initial fit parameters before setting them all free for a stable final fit. The results of the fit demonstrate that the stretching parameter of the slow process has a value of $\alpha_{slow} \sim 0.5 \pm 0.05$ with no significant dependence on temperature or hydration. The fastest process, that has been observed only at hydrations of $h \sim 0.3$ and higher, has weak stretching with $\alpha_{fast} \sim 0.9$. The main dielectric process exhibits the strongest stretching. It has a value of $\alpha_{main} \sim 0.4$−$0.3$ at $h \sim 0.37$, which tends to decrease down to $\alpha_{main} \sim 0.2$ in dehydrated samples. The characteristic relaxation times of all of the processes were obtained as the inverse of the frequency maximum in the fit $\varepsilon''(\nu)$ spectra, $\tau = (2\pi\nu_{max})^{-1}$ (this value is provided directly by the WINFit software from Novocontrol). We emphasize that the final fit has been also done using a Havriliak-Negami distribution function. However, the asymmetry parameters of all three processes were close to 1. This justifies the use of CC

distribution functions, although it does not exclude a possible weak asymmetry of the relaxation peaks.

**Acknowledgment.** We acknowledge partial financial support from NSF Polymer Program (DMR-0605784 and DMR-0804571).

## References and Notes

(1) Rupley, J. A.; Careri, G. *Adv. Protein Chem.* **1991**, *41*, 37–172.
(2) Frauenfelder, H.; Fenimore, P. W.; McMahon, B. H. *Biophys. Chem.* **2002**, *98*, 35–48.
(3) Gregory, R. B. *Protein-Solvent Interactions*; Marcel Dekker, Inc: New York, 1995.
(4) Rupley, J. A.; Yang, P.-H.; Tollin, G. *ACS Symp. Ser.* **1980**, *127*, 111–132.
(5) Ansari, A.; Jones, M. C.; Henry, E. R.; Hofrichter, J.; Eaton, W. A. *Science* **1992**, *256*, 1796–1798.
(6) Ansari, A.; Jones, C. M.; Henry, E. R.; Hofrichter, j.; Eaton, W. A. *Biochemistry* **1994**, *33*, 5128–5145.
(7) Caliskan, G.; Mehtani, D.; Roh, J. H.; Kilsliuk, A.; Sokolov, A. P.; Azzam, S.; Cicerone, M. T.; Lin-Gibson, S.; Peral, I. *J. Chem. Phys.* **2004**, *121*, 1978–1983.
(8) Krushelnitsky, A.; Reichert, D. *Prog. Nucl. Magn. Reson. Spectrosc.* **2005**, *47*, 1–25.
(9) Buck, M.; Boyd, J.; Redfield, C.; MacKenzie, D. A.; Jeenes, D. J.; Archer, D. B.; Dobson, C. M. *Biochemistry* **1995**, *34*, 4041–4055.
(10) Fitter, J.; Gutberlet, T.; Katsaras, J. *Neutron Scattering in Biology*; Springer: Berlin, 2006.
(11) Nandi, N.; Bhattacharyya, K.; Bagchi, B. *Chem. Rev.* **2000**, *100*, 2013–2045.
(12) Miura, N.; Hayashi, Y.; Mashimo, S. *Biopolymers* **1996**, *39*, 183–187.
(13) Oleinikova, A.; Sasisanker, P.; Weingartner, H. *J. Phys. Chem. B* **2004**, *108*, 8467–8474.
(14) Jansson, H.; Bergman, R.; Swenson, J. *J. Phys. Chem. B* **2005**, *109*, 24134–24141.
(15) Doster, W.; Cusack, S.; Petry, W. *Nature* **1989**, *337*, 754–756.
(16) Tsai, A. M.; Neumann, D. A.; Bell, L. N. *Biophys. J.* **2000**, *79*, 2728–2732.
(17) Sokolov, A. P.; Roh, J. H.; Mamontov, E.; García Sakai, V. *Chem. Phys.* **2008**, *345*, 212–218.
(18) Khodadadi, S.; Pawlus, S.; Roh, J. H.; Garcia Sakai, V.; Mamontov, E.; Sokolov, A. P. *J. Chem. Phys.* **2008**, *128*, 195106/1–195106/5.
(19) Roh, J. H.; Curtis, J. E.; Azzam, S.; Novikov, V. N.; Peral, I.; Chowdhuri, Z.; Gregory, R. B.; Sokolov, A. P. *Biophys. J.* **2006**, *91*, 2573–2588.
(20) Chen, S.-H.; Liu, L.; Fratini, E.; Bagliono, P.; Faraone, A. *Proc. Natl. Acad. Sci.* **2006**, *103*, 9012–9016.
(21) Swenson, J.; Jansson, H.; Hedstroem, J.; Bergman, R. *J. Phys.: Condens. Matter* **2007**, *19*, 205109/1−9.
(22) Swenson, J.; Jansson, H.; Bergman, R. *Rev. Lett. Phys.* **2006**, *96*, 247802/1–247802/4.
(23) Pethig, R. *Annu. Rev. Phys. Chem.* **1992**, *43*, 177–205.
(24) Oleinikova, A.; Smolin, N.; Brovchenko, I. *Biophys. J.* **2007**, *93*, 2986–3000.
(25) Tarek, M.; Tobias, D. J. *Phys. Rev. Lett.* **2002**, *88*, 138101/1–138101/4.
(26) Modig, K.; liepinsh, E.; Otting, G.; Halle, B. *J. Am. Chem. Soc.* **2004**, *126*, 102–114.
(27) Marchi, M.; Stapone, F.; Ceccarelli, M. *J. Am. Chem. Soc.* **2002**, *124*, 6787–6791.
(28) Sengupta, D.; Behera, R. N.; Smith, J. C.; Ullmann, G. M. *Structure* **2005**, *13*, 849–855.
(29) Zaccai, G. *Science* **2000**, *288*, 1604–1607.
(30) Lee, A. L.; Wand, J. *Nature* **2001**, *411*, 501–504.
(31) Parak, F. G. *Rep. Prog. Phys.* **2003**, *66*, 103–129.
(32) Daniel, R. M.; Smith, J. C.; Ferrand, M.; Héry, S.; Dunn, R.; Finney, J. L. *Biophys. J.* **1998**, *75*, 2504–2507.
(33) Fenimore, P. W.; Frauenfelder, H.; McMahon, B. H.; Young, R. D. *Proc. Natl. Acad. Sci. U.S.A.* **2004**, *101*, 14408–14413.
(34) Chu, X.; Fratini, E.; Baglioni, P.; Faraone, A.; Chen, S.-H. *Phys. Rev. E* **2008**, *77*, 011908/1–011908/6.
(35) Chen, S.-H.; Liu, L.; Chu, X.; Zhang, y.; Fratini, E,; Baglioni, P.; Faraone, A.; Mamontov, E. *J. Chem. Phys.* **2006**, *125*, 171103/1–171103/4.
(36) Bielowka, S. H.; Psurek, T.; Ziolo, J.; Paluch, M. *Phys. Rev. E* **2001**, *63*, 062301/1–062301/4.
(37) Egelstaff, P. A. *An Introduction to the Liquid State*; Clarendon: Oxford, U.K., 1992.
(38) Pawlus, S.; Khodadadi, S.; Sokolov, A. P. *Phys. Rev. Lett.* **2008**, *100*, 108103/1–108103/4.
(39) Roh, J. H.; Novikov, V. N.; Gregory, R. B.; Curtis, J. E.; Chowdhuri, Z.; Sokolov, A. P. *Phys. Rev. Lett.* **2005**, *95*, 038101/1–038101/4.
(40) Perez, J.; Zanotti, J.-M.; Durand, D. *Biophys. J.* **1999**, *77*, 454–469.
(41) Doster, W.; Settles, M. *Biochim. Biophys. Acta* **2005**, *1749*, 173–186.
(42) Krishnan, M.; Kurkal-Siebert, V.; Smith, J. C. *J. Phys. Chem. B* **2008**, *112*, 5522–5533.
(43) Andrew, E. R.; Bryant, D. J.; Cashell, E. M. *Chem. Phys. Lett.* **1980**, *69*, 551–554.
(44) Daniel, V. V. *Dielectric Relaxation*; Academic Press: London and New York, 1967.

JP8059807